Proceedings of the Fortieth National Conference on Fluid Mechanics and Fluid Power
December 12-14, 2013, NIT Hamirpur, Himachal Pradesh, India

FMFP 2013 Paper 170

NUMERICAL ANALYSIS OF TRANSITIONAL FLOW PAST FLAT PLATE

A. Rajesh
Project Assistant, CSIR-NAL
Bangalore, India
rajeshamech@gmail.com

Dattatraya. S. Kulkarni
Sr. Scientist, CSIR-NAL
Bangalore, India
kulkarni@ctfd.cmmacs.ernet.in

B. N. Rajani
Principal Scientist, CSIR-NAL
Bangalore, India
rajani@ctfd.cmmacs.ernet.in

ABSTRACT

Prediction of flow transition plays an important role in the design and performance of aerospace devices and turbomachinery applications. The correlation based transition modeling is one of the commonly used approaches to predict transition, as these can be easily adapted into any general CFD code. In the present study, Abu-Ghannam and Shaw (AGS) empirical correlation based transition model available in the literature, have been successfully implemented in the in-house code 3D-PURLES. The AGS correlation based transition model coupled to turbulence models available in 3D-PURLES have been validated for flat plate with zero, adverse and favourable pressure gradients.

Key Words: Flat plate, intermittency, correlation based transition modelling, Abu-Ghannam and Shaw correlation, SA turbulence model

INTRODUCTION

Transition is a complex phenomenon defining the process of the laminar flow changing to turbulent flow. There are three important modes of transition *viz.* natural transition, bypass transition and separated flow transition. The natural transition process is initiated by the formation of weak instabilities in the laminar boundary layer. These instabilities amplify and proceed through various stages until they develop in to a fully turbulent flow. The bypass transition usually occurs when the freestream turbulence is high causing the formation of the turbulent spots in the boundary layer bypassing the initial stages of natural transition process. This process is caused due to the disturbances in external flow such as freestream turbulence. The separated flow transition occurs in the separated flow region within the shear layer and the process is similar to natural transition.

Flow transition plays an important role in the design and performance of aerospace devices and turbomachinery applications where the wall shear stress or the wall heat transfer is of interest. The transition can also have large positive effect on MAVs (Micro Air Vehicles), since these operate at low Reynolds number regimes, where the flow is dominated by large viscous effects which are associated with thick boundary layers resulting in higher viscous drag and lower maximum lift.

MATHEMATICAL MODELLING

The time-averaged Navier Stokes equations for unsteady incompressible flow in the coordinate-free form is written as follows,

$$\nabla . \rho \boldsymbol{U} = 0$$

$$D_t \rho \boldsymbol{U} = -\nabla P + \nabla . \left((\mu + \mu_t)(\nabla \boldsymbol{U} + \nabla^t \boldsymbol{U}) \right)$$

Where μ and ρ are fluid viscosity and density, p and $\boldsymbol{U}$ are the time-averaged pressure and velocity vector respectively. The eddy viscosity μ_t is evaluated through different turbulence models and D_t represents the total derivative with respect to time. In order to handle transitional flows, Abu-Ghannam and Shaw (AGS) empirical correlation based transition model available in the literature, has been successfully implemented and coupled to SA (Spalart-Allmaras) turbulence model available in 3D-PURLES.

Transition Modeling

The present work uses an empirical correlation proposed by Abu-Ghannam and Shaw 1980 to determine the transition onset location (*Xs*), the length of transition zone and intermittency factor (γ). In the laminar region, the intermittency factor is set to zero, varies between zero and one in the transitional region and attains a value of one in the fully turbulent region. The intermittency factor which is the function of streamwise direction ($\gamma(x)$) is multiplied with eddy viscosity (μ_t). The intermittency function $\gamma(x)$ is obtained by using the following function

$$\gamma(x) = 1 - exp(-5\eta^3) \qquad (1)$$

where, η is non-dimensional transition length parameter and is given by

$$\eta = \frac{Re_X - Re_{Xs}}{Re_{Xe} - Re_{Xs}} \qquad (2)$$

where $Re_x = \frac{\rho x U_\infty}{\mu}$ is Reynolds number based on flat plate length (x) and freestream velocityU_∞, Re_{Xs} is Reynolds number based on length at start of transition (*Xs*). The transition onset location *Xs* is fixed when the local momentum thickness based Reynolds number (Re_θ) exceeds the correlation given by Abu Ghannam and Shaw (Eq. 3).

$$Re_{\theta s} = 163 + exp\left\{F(\lambda_\theta) - \frac{F(\lambda_\theta)}{6.91}Tu\right\} \qquad (3)$$

where $F(\lambda_\theta)$ is obtained using the following expression

$$F(\lambda_\theta) = 6.91 + 12.75(\lambda_\theta) + 63.64(\lambda_\theta)^2$$

where $\lambda_\theta < 0$

$$F(\lambda_\theta) = 6.91 + 2.48(\lambda_\theta) - 12.27(\lambda_\theta)^2$$

where $\lambda_\theta > 0$

where, $\lambda_\theta = \frac{\theta^2}{\nu}\frac{dU_e}{dx}$ is pressure gradient parameter and U_e is velocity at edge of boundary layer.

Based on the onset Reynolds number (Re_{Xs}), the Reynolds number (Re_{Xe}) at the end of transition location (X_e) is determined using the following relation.

$$Re_{Xe} = Re_{Xs} + 16.8Re_{Xs}^{0.8} \qquad (4)$$

Numerical Method

The present computation uses a general geometry, multi-block structured, pressure-based implicit finite volume algorithm 3D-PURLES, developed at the CTFD Division, CSIR-NAL Bangalore to solve the unsteady turbulent incompressible flow. The details of the iterative decoupled approach used to handle the pressure-velocity link of the governing equations are given in (Majumdar et al., 2009).

COMPUTATIONAL DETAILS

The boundary conditions used for zero, adverse and favourable pressure gradient flat plate cases are shown in Fig. 1. Based on grid sensitivity study carried out, 174 grid nodes along stream-wise direction and 101 grid nodes in cross-stream direction with grids stretched towards the wall in order to resolve the boundary layer have been used for zero pressure gradient cases. For the non-zero pressure gradient cases the grid size in the cross-flow direction

has been doubled in order to resolve the tunnel boundary layer and to maintain the same resolution near plate wall. For all the cases, the wall normal distance of the first grid point is maintained at 1×10^{-6} in order to obtain near wall non-dimensionalised distance of $y^{+}<1$. The convergence criterion (CC) has been fixed to be $10^{-4.}$ At the inlet plane of flat plate a uniform inlet velocity profile and at the outlet plane, convective boundary condition (U=Dϕ/Dt=0) are specified. The simulations have been carried out using third order accurate QUICK scheme for the convective flux discretisation.

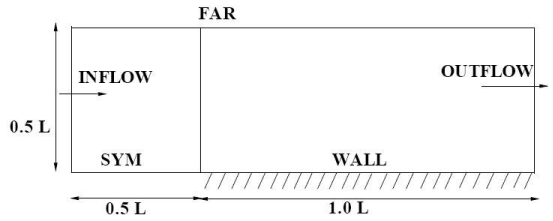

(a) Zero pressure gradient case

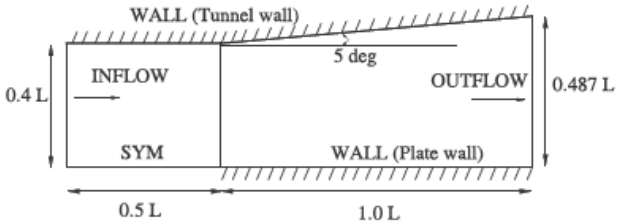

(b) Adverse pressure gradient case

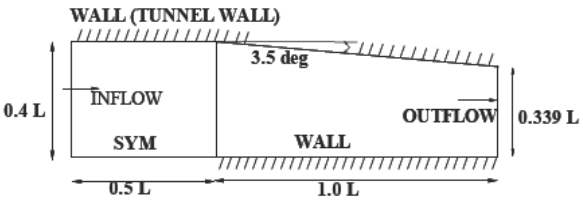

(c) Favourable pressure gradient case

Figure 1. Boundary conditions used for flat plate simulations

RESULTS AND DISCUSSIONS

Flow analysis for flat plate with zero pressure gradient have been carried out for different test cases *viz.* Savill 1993, Abu-Ghannam & Shaw 1980 and Dhawan & Narasimha (DN) 1958. Analyses have also been carried out for adverse and favourable pressure gradient test case of AGS. The paper however discusses only the results obtained for AGS and DN test cases.

Zero Pressure Gradient (ZPG)

The simulation have been carried out for DN case (*Re* = 11, 72, 000, *Tu* = 1.3%) and AGS case (*Re* = 17, 58, 000 and *Tu* = 1.25%) using Spalart Allmaras + Transition correlation (SA+TC) model. The computed skin friction coefficient (C_f) is compared with corresponding measurement data and is shown in Fig. 2 and Fig. 3 respectively. The figures clearly indicate that SA model coupled with transition correlation closely matches with the measurement data.

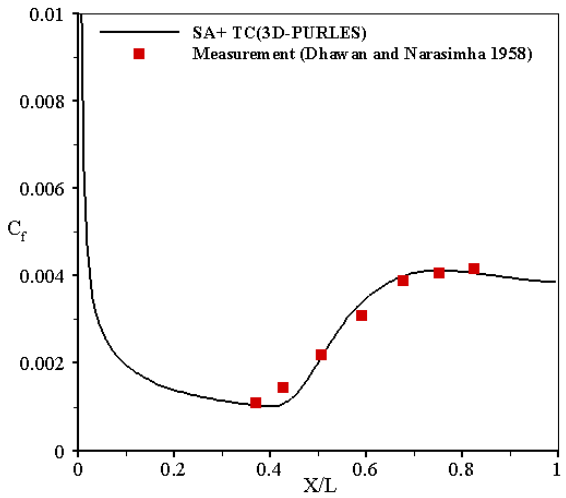

Figure 2. Variation of C_f along the flat plate (ZPG) for DN test case

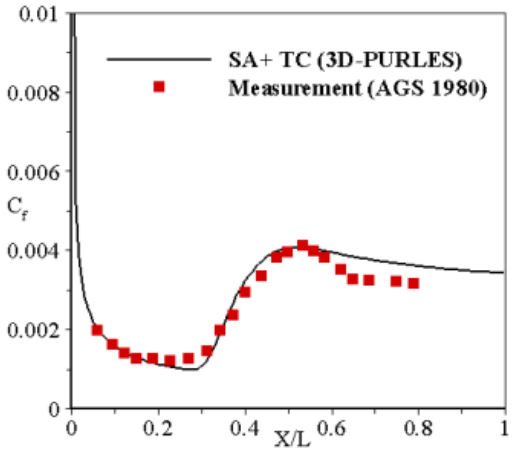

Figure 3. Variation of C_f along the flat plate (ZPG) for AGS test case

Adverse Pressure Gradient (APG)

In the absence of exact tilt angle used in the experiments, simulations have been carried out for different tilt angles. The comparison of the computed pressure coefficient ($C_p = \left(P - P_{ref}\right)/0.5\rho u_{ref}^2$ where P_{ref} is the reference static pressure measured at X/L = 0.95 where L is length of the flat plate) with measurement data (Fig. 4.) indicates that measurements have been carried out at tilt angle close to 5°.

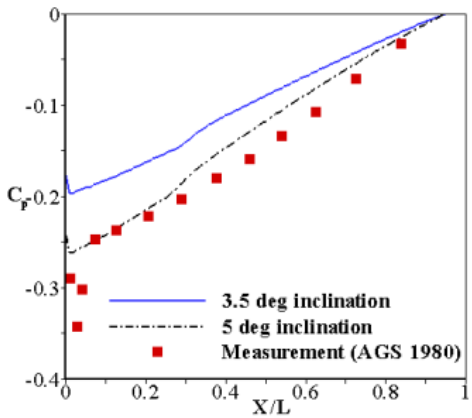

Figure 4. Pressure distribution for different angle of inclination

The computed skin friction coefficient obtained using SA+TC for 5° inclination is compared with measurement data as shown in Fig. 5. A good agreement between the present computation and measurement is observed for the C_f distribution in the laminar and transition regions. In spite of the good agreement with the measurement data for the location of onset of transition (Xs = 0.22), the C_f obtained with the present simulation is observed to be underpredicted in the fully turbulent region. The discrepancies observed in fully turbulent region may be attributed to the fact that in this simulation the tunnel wall has been restricted only up to the tilt wall.

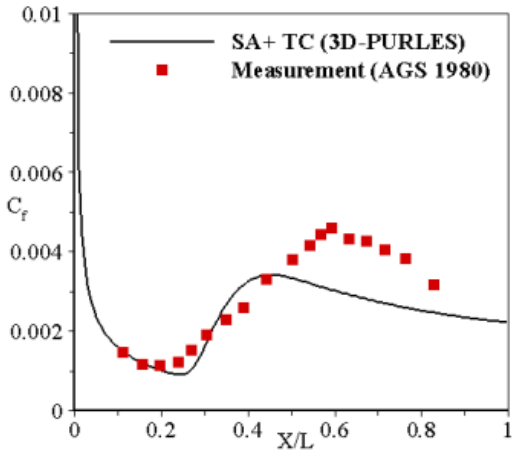

Figure 5.Variation of C_f along the flat plate for APG case

Favourable Pressure Gradient (FPG)

Similar to adverse pressure gradient case, different angles of tilt were tried in order to arrive at the tilt angle used in the experiments by comparing the pressure coefficient distribution (Fig. 6). The figure clearly indicates that the C_p obtained for -3.5° tilt matches closely with measurement data indicating that in the experimental setup the tunnel wall was inclined approximately at -3.5°.

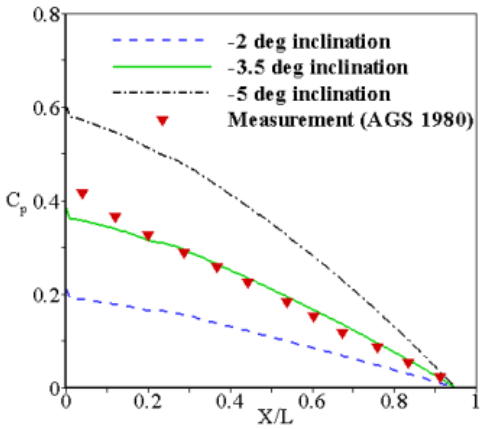

Figure 6. Pressure coefficient distribution for different angle of inclination

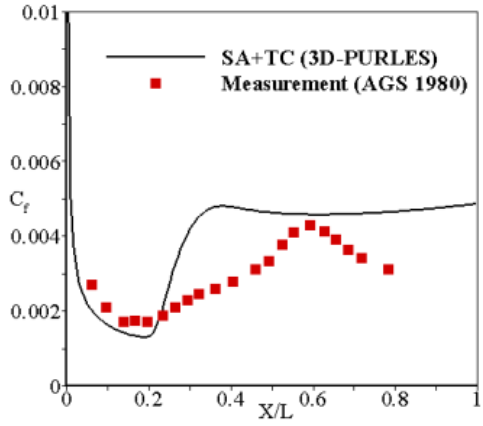

Figure 7. Variation of C_f along the flat plate for FPG case

The comparison of the skin friction coefficient distribution obtained using SA+TC for -3.5^o is shown in Fig. 7 which clearly indicates that the computation has underpredicted the transition onset location (*Xs* = 0.17) as well as the length of the transition when compared to the measurement (*Xs* = 0.2). The reason for the discrepancy in predicting the length of the transition may be mainly attributed to the fact that the correlation used is unable to mimic the influence of the favourable pressure gradient. Generally in the favourable pressure gradient the flow remains laminar for a longer period and hence increasing the transition region and shortening the fully turbulent region. This phenomenon is captured by the experiments where as the present correlation based transition model predicts a steep change from laminar region to turbulent.

CONCLUSION

The Abu-Ghannam and Shaw transition correlation model has been incorporated in the 3D-PURLES code and successfully coupled to the SA turbulence model. The correlation based transition model has been validated for flat plate test cases with zero and non-zero pressure gradients having different Reynolds number and turbulence intensities. For zero pressure gradient test cases of AGS and DN a very good agreement with the measurement has been observed for the skin friction coefficient. In the adverse pressure gradient test case, the computed skin friction coefficient in the laminar and transition region follows the experiments closely and in the turbulent region it is observed to be underpredicted. On the other hand, in the favourable pressure gradient case the transition length itself is underpredicted by the present correlation model leading to a significant difference in the skin friction value in the transition and fully turbulent regions. The present correlation based transition model is generally applicable only to non-separated flows. In order to handle transition in separated flows we need to look at more sophisticated models which are based on transport equations.

ACKNOWLEDGMENTS

The authors wish to express their heartfelt thanks to the Head CTFD Division, CSIR-NAL, Bangalore for his support. We also deeply thank Director CSIR-NAL, Bangalore for his permission to publish this paper.

NOMENCLATURE

3D-PURLES	-	Three Dimensional- Pressure based Unsteady RANS LES Solver
AGS	-	Abu-Ghannam and Shaw
APG	-	Adverse Pressure Gradient
CC	-	Convergence Criterion
C_f	-	Skin friction coefficient
C_p	-	Pressure coefficient
DN	-	Dhawan & Narasimha
FPG	-	Favourable Pressure Gradient
L	-	Length of flat plate
MAV	-	Micro Air Vehicles
P_{ref}	-	Reference static pressure
QUICK	-	Quadratic Upwind interpolation for Convection Kinematics
Re_x	-	Length based Reynolds number
$Re_{\theta s}$	-	Momentum based Reynolds number at the start of transition
Re_θ	-	Momentum based Reynolds number
Re_{xs}	-	Length based Reynolds number at the start of transition
Re_{xe}	-	Length based Reynolds number at the end of transition
SA	-	Spalart-Allmaras
SA+TC	-	Spalart-Allmaras + Transition Correlation
Tu	-	Turbulent Intensity
U_e	-	Velocity at edge of boundary layer
Xs	-	Transition Onset Location
y^+	-	Non-dimensionalised near wall distance
ZPG	-	Zero Pressure Gradient
γ	-	Intermittency factor
η	-	Non-dimensional transition length
λ_θ	-	Pressure gradient parameter
μ	-	Fluid viscosity
μ_t	-	Eddy viscosity
θ	-	Momentum Thickness
ρ	-	Density

REFERENCES

Savill, A. M., 1993. Some recent progress in the turbulence modelling of by-pass transition, Near wall turbulent flows, Elsevier.

Abu-Ghannam, B. J., Shaw, R., 1980. Natural transition of boundary layers -the effects of turbulence, Pressure gradient, and flow history. Journal of Mechanical Engineering Science, (22) 213–228.

Dhawan, S., Narasimha, R., 1958. Some properties of boundary layer during the transition from laminar to turbulent flow motion . Journal of Fluid Mechanics, (3) 418–436.

Majumdar, S., Rajani, B. N., Kulkarni, D. S., Subrahmanya, M. B., 2009. CFD simulation of low speed turbulent flow problems using unsteady RANS and Large Eddy Simulation approach Journal of Aerospace Sciences and Technologies,(61)111–122.